

Published in final edited form as:

Arterioscler Thromb Vasc Biol. 2012 June ; 32(6): 1383–1391. doi:10.1161/ATVBAHA.112.248922.

Reactive Oxygen Species Regulate Osteopontin Expression in a Murine Model of Post-Ischemic Neo-vascularization

Alicia N. Lyle¹, Giji Joseph¹, Aaron E. Fan¹, Daiana Weiss¹, Natalia Landázuri¹, and W. Robert Taylor^{1,2,3}

¹Department of Medicine, Division of Cardiology, Emory University School of Medicine, Atlanta, Georgia 30322

²The Wallace H. Coulter Department of Biomedical Engineering, Emory University School of Medicine and Georgia Institute of Technology, Atlanta, GA

³Cardiology Division, Atlanta Veterans Affairs Medical Center, Atlanta, GA

Abstract

Objective—Previous findings from our laboratory demonstrated that neo-vascularization was impaired in osteopontin (OPN) knockout animals. However, the mechanisms responsible for regulation of OPN expression in the setting of ischemia remain undefined. Therefore, we sought to determine if OPN is upregulated in response to ischemia and hypothesized that H₂O₂ is a critical component of the signaling mechanism by which OPN expression is upregulated in response to ischemia *in vivo*.

Methods and Results—To determine if ischemic injury upregulates OPN, we used a murine model of hind limb ischemia. Femoral artery ligation in C57Bl/6 mice significantly increased OPN expression and H₂O₂ production. Infusion of C57Bl/6 mice with PEG-catalase (10,000 U/kg/day) or the use of transgenic mice with smooth muscle cell specific catalase overexpression blunted ischemia-induced OPN, suggesting ischemia-induced OPN expression is H₂O₂-dependent. Decreased H₂O₂-mediated OPN blunted reperfusion and collateral formation *in vivo*. In contrast, the overexpression of OPN using lentivirus restored neovascularization.

Conclusions—Scavenging H₂O₂ blocks ischemia-induced OPN expression, providing evidence that ischemia-induced OPN expression is H₂O₂-dependent. Decreased OPN expression impaired neo-vascularization, whereas overexpression of OPN increased angiogenesis, supporting our hypothesis that OPN is a critical mediator of post-ischemic neo-vascularization and a potential novel therapeutic target for inducing new vessel growth.

Keywords

Osteopontin; Reactive Oxygen Species; Ischemia; Angiogenesis; Collateral Circulation

The occlusion of blood vessels ultimately leads to ischemia, initiating multiple processes that promote neo-vascularization as a compensatory mechanism to restore blood flow and

Address correspondence to: W. Robert Taylor, M.D., Ph.D. Emory University School of Medicine, Division of Cardiology 1639 Pierce Drive, Suite 319 WMB, Atlanta, GA 30322. wtaylor@emory.edu Phone: 404.727.8921; Fax: 404.727.3330.

Disclosures None.

This is a PDF file of an unedited manuscript that has been accepted for publication. As a service to our customers we are providing this early version of the manuscript. The manuscript will undergo copyediting, typesetting, and review of the resulting proof before it is published in its final citable form. Please note that during the production process errors may be discovered which could affect the content, and all legal disclaimers that apply to the journal pertain.

preserve tissue function. The ability to develop new collaterals is strongly associated with reduced long-term cardiac mortality in patients with acute myocardial infarction and stable coronary artery disease.¹ The formation of new collaterals is a multi-factorial process that requires cytokines, the infiltration of inflammatory cells, cell proliferation, cell migration, and matrix remodeling. Several of these processes are modulated by the presence of osteopontin (OPN),^{2,3} a secreted, phosphorylated matricellular protein critical for neo-vascularization.^{4,5}

OPN is important for normal arterial physiology⁶ and is expressed by multiple cell types including monocytes/macrophages, endothelial cells, and smooth muscle cells (SMCs),⁷ all of which play a role in the neo-vascularization process. OPN mediates several processes relevant to collateral formation, including cell survival,⁸ cell adhesion,^{9,10} and migration.^{9,11} Additionally, wound healing, a process that requires angiogenesis, is significantly impaired in OPN^{-/-} mice,^{4,12} strongly supporting a role for OPN in angiogenesis. Moreover, our group previously demonstrated a direct role for OPN in post-ischemic neo-vascularization by showing dramatically impaired collateral formation in OPN^{-/-} mice compared to wild-type controls in a murine model of hind limb ischemia (HLI).⁵

OPN is a non-collagenous, phosphorylated glycoprotein thought to mediate cellular functions by providing a link between cell surface receptors and structural extra-cellular matrix molecules.¹³ OPN functions in a variety of biological processes and signals by binding to cell surface integrins through a conserved RGD domain or the SVVYGLR binding domain, which is exposed when OPN is cleaved by thrombin or MMPs.¹³ OPN is also a ligand for the CD44 receptor.¹⁴ Additionally, OPN promotes the migration of multiple cell types, including macrophages,¹⁵ endothelial cells,^{9,10} and vascular smooth muscle cells.^{9,10,16} An alternative translation start site in the OPN messenger RNA generates two OPN isoforms: a secreted form and an intracellular form (iOPN).¹⁷ Both secreted and intracellular OPN are linked to cell migration, where iOPN localizes to the cell membrane and associates with CD44¹⁸ and secreted OPN regulates cell responses through association with integrin receptors and the CD44 receptor.

Reactive oxygen species (ROS), such as superoxide (O₂^{•-}) and hydrogen peroxide (H₂O₂), are involved in physiological and pathophysiological responses. When produced in excess, ROS promote cell injury and disease pathologies. In contrast, at physiologic levels, ROS function as second messengers and regulate redox signaling pathways that modulate cell migration, proliferation, and matrix remodeling, all of which are necessary events for neovascularization.¹⁹⁻²² A recent study by Tojo, et. al. provided a direct link between NADPH oxidases and post-ischemic neo-vascularization in a murine model of HLI. The study demonstrated that animals lacking gp91phox, a subunit of the Nox2 NADPH oxidase, produce less ROS and form fewer collaterals compared to wild-type animals.²³

While several recent publications link ROS to OPN expression *in vitro*,²⁴⁻²⁶ little is known regarding the role of ROS in regulating OPN expression *in vivo*. Furthermore, the precise molecular identity of the relevant ROS remains unclear. The goals of this study were to determine if OPN is upregulated in response to ischemia, if increased ROS production is the mechanism by which OPN expression is increased, and to define the molecular identity of the relevant ROS involved in OPN expression *in vivo*. In this study, we demonstrate that OPN is upregulated in response to ischemia using a murine model of hind limb ischemia. Femoral artery ligation in C57Bl/6 mice significantly increased OPN expression and H₂O₂ production in the ischemic leg (IL), compared to the non-ischemic leg (NIL). Using pharmacologic and transgenic approaches to scavenge H₂O₂, we demonstrate that ischemia-induced OPN expression is H₂O₂-dependent. Infusion of mice with PEG-catalase (10,000 U/

kg/day) or the use of transgenic mice with SMC-specific catalase overexpression (Tg^{SMC-Cat}) significantly blunted ischemia-induced OPN expression, resulting in delayed reperfusion and impaired collateral formation in response to ischemia. In addition, using the same model of Tg^{SMC-Cat} mice, when we utilized lentiviral delivery to overexpress OPN in the ischemic limb, we were able to completely restore neo-vascularization in the ischemic limb. Altogether, the results presented herein define a novel mechanism for the regulation of OPN expression *in vivo*, establish an absolute requirement for H₂O₂-dependent OPN for effective collateral formation, and support the concept that OPN is a critical mediator of neo-vascularization. Therefore, OPN may be a novel therapeutic target for promoting collateral vessel formation.

MATERIALS and METHODS

A detailed, expanded Materials and Methods section is available in the online data supplement at <http://circres.ahajournals.org>.

Animals

Male C57BL/6 mice were purchased from Jackson Laboratories (Maine, USA). Tg^{SMC-Cat} mice were bred in house in the Department of Animal Resources at Emory University. Tg^{SMC-Cat} mice have increased expression of human catalase through the SMC-specific smooth muscle myosin heavy chain (MHC) promoter and were characterized previously.²⁷ For all experiments Tg^{SMC-Cat} mice were compared to wild-type littermates. In some experiments, PEG-Catalase (10,000 U/kg/day) dissolved in saline was delivered by intravenous infusion via osmotic mini-pump. PEG-catalase was infused continuously from time of HLI surgery until the designated time points. All animals used were male and between 8 and 10 weeks of age. The animals were housed and cared for according to the guidelines approved by the Emory University Institutional Animal Care and Use Committee.

Osmotic Mini-pump Implantation

Mice were anesthetized using 3% isoflurane (oxygen delivered at 0.5L/min with 3% isoflurane for induction and 2.0% isoflurane for maintenance). A catheter attached to a primed osmotic mini-pump (Alzet osmotic mini-pump, model 1007D, Durect Corporation, Cupertino, CA) was inserted into the jugular vein and the pump inserted subcutaneously. Mice were administered buprenex (0.01-0.1mg/kg, SC) as needed.

Hind Limb Ischemia Surgery

Mice were anesthetized with 3% isoflurane in a chamber and then anesthetized with 2% isoflurane through a nose cone. Ligation and excision of the left superficial femoral artery was performed as described previously.^{5, 28}

LASER Doppler Perfusion Imaging

LASER Doppler perfusion imaging (LDPI) was performed as described previously.^{5, 28} Briefly, mice were anesthetized by inhalation of 2% isoflurane and scanned with the LDPI system (PIM II LASER Doppler Perfusion Imager). Perfusion of the proximal region was quantified and normalized to the non-surgical limb.

Micro-CT Imaging

Quantitative micro-CT was used for evaluation of collateral vessel formation in the ischemic limb at postoperative day 5 as described previously.^{5, 28} Briefly, mice were euthanized (n=6-9 for each group) and sequentially perfused with saline containing 4 mg/mL of papaverine, 10% formalin, followed by a lead chromate-based contrast agent (Flow Tech,

Inc, South Windsor, CT). Bone was de-mineralized in a formic acid based solution (Cal-Ex II, Fisher Scientific, Pittsburgh, PA) for 48 hours. Samples were then imaged at a 30 μ m voxel size, and the tomograms were used to render binarized 3-D images. Stereological algorithms were used to quantify vascular volume to tissue volume ratio, connectivity, and vascular density, which were then normalized to the contralateral control limb.

Lentivirus

The lentiviral vector was derived from the HIV-based lentivirus backbone pLV-CMVGFP-U3Nhe, as described previously.²⁹⁻³¹ pLV-CMV-GFP-U3Nhe control vector will hereafter be referred to as LV-GFP. We generated a dual-tagged human osteopontin construct with an HA-tag at the N-terminus and myc-tag at the C-terminus. We inserted a wild-type internal ribosome entry site (IRES),³² followed by dual-tagged OPN, downstream of GFP to generate a lentivirus that expresses both GFP and tagged OPN, hereafter referred to as LV-OPN. The wild-type IRES used allows high translation of the downstream compared to the upstream coding sequence in the same mRNA,³² thereby allowing the final construct to express high OPN and relatively lower GFP protein.

Viral production procedures have been described in detail previously.^{29, 33, 34} For *in vivo* use, both lentiviruses were used at a final concentration of $\sim 1 \times 10^9$ infectious particles/mL. All animals received HLI, after which the IL adductor was injected with 20 μ L of LV-GFP or LV-OPN lentivirus using a similar approach as that described previously.²⁹

Detection of ROS

The production of O₂^{•-} was evaluated by measuring the conversion of DHE to 2-hydroxyethidium using HPLC, as described previously.³⁵ Superoxide production was normalized to protein concentration. H₂O₂ production was measured using the Amplex Red Assay (Invitrogen, Carlsbad, CA), as described previously.³⁵ H₂O₂ production was normalized to tissue wet weight.

Immunofluorescence

Mice were sacrificed and tissues were perfused with saline and fixed with 10% buffered formalin. Sections from paraffin embedded hind limbs were cut in 5 μ m increments. Antigen retrieval was performed in citrate buffer, pH 6.0 (Invitrogen, Carlsbad, CA), prior to incubation with OPN antibody (1:200 in 3% BSA), followed by incubation with anti-mouse or anti-goat secondary antibody (1:400 in 3% BSA; Vector Labs, Burlingame, CA), and incubation with Streptavidin QDot 655 (1:200 in 3% BSA; Invitrogen, Carlsbad, CA). Images were acquired on a Zeiss Axioskop microscope equipped with an AxioCam camera.

Immunoblotting

Adductor muscle tissues and cultured SMCs were lysed in Hunter's buffer.³⁵ Briefly, tissues were homogenized with glass mortar and pestle and cell samples were sonicated at 10 watts for 10 seconds. Whole tissue or cell lysates were used for immunoblotting. The osteopontin antibodies used were from Santa Cruz Biotechnology (Santa Cruz, CA) and R&D Systems (Minneapolis, MN). GAPDH antibody was also obtained from Santa Cruz Biotechnology (Santa Cruz, CA). The β -actin antibody was from Cell Signaling (Danvers, MA). Band intensity was quantified by densitometry using ImageJ 1.38 software and expressed/normalized to β -actin or GAPDH.

Cell Culture

Murine aortic SMCs (passages 4-10) were cultured in low-glucose Dulbecco's Modified Eagle's Media (DMEM; Sigma Aldrich, Saint Louis, MO) supplemented with 10% fetal

bovine serum (FBS; Sigma Aldrich, Saint Louis, MO), 2 mM L-glutamine, 100 units/mL penicillin, and 100 µg/mL streptomycin, all acquired from Mediatech, Inc. (Manassas, VA). Cells were stimulated with H₂O₂ (Sigma Aldrich, Saint Louis, MO) after 48 hours of quiescence in serum-free DMEM for all experiments.

RNA Isolation and Quantitative RT-PCR

Total RNA was extracted from muscle tissue or cells using the RNeasy kit (Qiagen, Valencia, CA). OPN and 18S rRNA, were measured by amplification of cDNA using the thermocycler (Applied Biosystems) and SYBR green dye. Copy number was calculated by the instrument software from standard curves of genuine templates. OPN copy number was normalized to 18S rRNA.

Statistical Analysis

Results are expressed as mean ± S.E.M. from at least three independent experiments. Statistical significance for quantitative results was assessed using analysis of variance (ANOVA), followed by Bonferroni's Multiple Comparison post-hoc test. In some cases, a Students' *t*-test was used to assess significance. A value of $p < 0.05$ was considered statistically significant.

RESULTS

Effects of Hind Limb Ischemia on Osteopontin Expression

Our previous study demonstrated that OPN^{-/-} mice exhibit impaired collateral formation.⁵ Therefore, we set out to determine if OPN is upregulated in response to ischemia by utilizing a murine model of HLI in which the femoral artery was ligated and excised, thus providing a stimulus for collateral formation. We measured OPN protein expression in the adductor muscles of the IL and NIL at 0, 3, 5, 7, 14, and 21 days post-HLI. As shown in Figure 1A, full-length (FL) OPN protein expression in the IL peaked between 5 and 7 days post-HLI, followed by a significant decline thereafter. Therefore, we investigated the effects of HLI on OPN expression at 5 days post-surgery. To evaluate if ischemia increases OPN mRNA levels, we used qRT-PCR to measure OPN message in the adductor muscles of the IL and NIL after 5 days. OPN mRNA levels were increased 20-fold in the IL compared to NIL (Figure 1B). OPN protein expression in the IL was also significantly increased compared to NIL, as measured by Western blot (WB) (Figure 1C) and immunofluorescence (IF) (Figure 1D). The ischemia-induced increases in OPN protein appeared as multiple bands by WB, presumably due to post-translational modification. Full-length OPN is a complex matricellular protein that is glycosylated, phosphorylated, and cleaved by other proteins after secretion into the extracellular space.³⁶ We detected an increase in both full-length, modified OPN (upper bands in 1C), as well as cleaved OPN (lower band in 1C).

Multiple cell types involved in the process of collateral formation are reported to express OPN in other systems. To determine the specific cell types that contribute to ischemia-induced increases in OPN expression at 5 days post-ischemia, we performed a series of immunofluorescence co-staining experiments. As shown in Figure 1D-E, multiple cell types express OPN in response to ischemia. OPN clearly co-localizes with Mac3 (Figure 1D), a marker of macrophages, with lectin (Figure 1E), a marker of endothelial cells, and with smooth muscle α -Actin (Figure 1F), a marker of SMCs. Taken together, these data demonstrate that ischemia increases OPN expression at the mRNA and protein levels, and that multiple cell types, including macrophages, endothelial cells, and smooth muscle cells, contribute to ischemia-induced increases in OPN expression.

Effects of Hind Limb Ischemia on Reactive Oxygen Species Production

To determine what ROS, if any, are increased in response to ischemic injury and to establish a time course for ROS production in this model, we used dihydroethidium (DHE)-HPLC and the Amplex Red Assay to measure $O_2^{\bullet-}$ and H_2O_2 production, respectively. ROS were measured in the adductor muscles of the NIL and IL of C57Bl/6 mice at postoperative days 3, 5, and 7. There were no detectable differences in $O_2^{\bullet-}$ between the IL and NIL at any time point (Figure 2A). In contrast, H_2O_2 production was significantly increased in response to ischemia at all time points (Figure 2B), with a peak in H_2O_2 at 5 days.

H_2O_2 Stimulates Osteopontin Expression In Vivo

Since we have demonstrated that in response to ischemia there is a significant increase in H_2O_2 and that OPN levels are increased in response to ischemia, we set out to determine if the increases in OPN are H_2O_2 -dependent. We performed HLI on C57Bl/6 mice infused with saline or PEG-catalase (10,000 U/kg/day), which converts H_2O_2 to water and other metabolites, thus diminishing H_2O_2 . PEG-catalase blunted ischemia-induced H_2O_2 production compared to saline infused animals (Figure 3A), as measured by Amplex Red Assay. This decrease in H_2O_2 production in the IL substantially blocked ischemia-induced OPN expression at the mRNA (Figure 3B). In addition, we found a similar corroborating result at the protein level when measured by WB and IF (Figure 3C & 3D). Taken together, these data support our hypothesis that the increase in OPN expression is response to ischemia is H_2O_2 -dependent.

Multiple cell types involved in ischemia-induced collateral formation express OPN in response to ischemia, including SMCs (Figure 1F). SMCs are also known to generate ROS and play a vital role in arteriogenesis. To confirm and further substantiate that ischemia-induced OPN expression is H_2O_2 -dependent, and to verify that SMCs may be a substantial contributor to H_2O_2 -dependent OPN expression in the ischemic hind limb, we utilized transgenic mice that overexpress catalase specifically in their SMCs ($Tg^{SMC-Cat}$). We then measured ROS and OPN expression in these mice. We found that $Tg^{SMC-Cat}$ mice have significantly diminished ischemia-induced H_2O_2 production compared to wild-type controls (Figure 4A). This decrease in H_2O_2 production mediated by SMC-specific catalase overexpression blunted ischemia-induced increases in OPN mRNA (Figure 4B). Additionally, OPN protein levels were substantially blunted in $Tg^{SMC-Cat}$ animals compared to wild-type controls, as measured by Western blot and IF (Figures 4C & 4D). Taken together, these data support that ischemia-induced OPN expression is H_2O_2 -dependent and that SMC-derived H_2O_2 significantly contributes to ROS-dependent OPN expression.

H_2O_2 -dependent OPN Mediates Collateral Formation

To determine the functional importance H_2O_2 and OPN on collateral formation, we used LDPI to evaluate reperfusion and Micro-CT to quantify collateral formation in the IL. LDPI images acquired at postoperative day 5 clearly illustrate that PEG-catalase infusion, which decreased ischemia-induced OPN expression and H_2O_2 levels, impaired reperfusion (Supplemental Figure 2A). Quantitative analysis illustrates a significant lag in perfusion recovery in the IL of PEG-catalase infused animals (Supplemental Figure 2B). Quantitative analysis of Micro-CT images (Supplemental Figure 2C) revealed PEG-catalase animals have a 19.4% reduction in vascular volume (saline 1.3 ± 0.1 vs. PEG-catalase 1.0 ± 0.1 ; normalized to tissue volume), 8.1% decrease in vascular density (saline 1.2 ± 0.03 vs. PEG-catalase 1.0 ± 0.02), and a 41.0% reduction in connectivity (saline 2.6 ± 0.40 vs. PEG-catalase 1.5 ± 0.2) compared to controls. Together, these data demonstrate that H_2O_2 increases OPN expression, which has a direct effect in the formation of collateral vessels after HLI injury.

To determine the functional importance SMC-derived H₂O₂ and OPN on collateral formation, we used LDPI to evaluate reperfusion and Micro-CT to quantify collateral formation in the IL of Tg^{SMC-Cat} animals using LDPI. Tg^{SMC-Cat} animals showed significantly decreased reperfusion compared to wild-type animals (Figure 5A-B). Quantitative analysis of Micro-CT images (Figure 5C) revealed Tg^{SMC-Cat} mice have a 34.6% reduction in vascular volume (WT 1.23±0.16 vs. Tg^{SMC-Cat} 0.81±0.06), 14.2% decrease in vascular density (WT 1.04±0.04 vs. Tg^{SMC-Cat} 0.89±0.04), and a 40.9% reduction in connectivity (WT 1.45±0.20 vs. Tg^{SMC-Cat} 0.85±0.09) compared to controls. Altogether, these data suggest that SMC-derived H₂O₂ significantly contributes to ROS-dependent OPN expression and neo-vascularization.

ROS influence the expression of several inflammatory factors in this model, including monocyte chemoattractant protein (MCP)-1 (Supplemental Figure 1), tumor necrosis factor (TNF)-α (Supplemental Figure 1), and OPN (Figures 3 & 4). Therefore, to determine the relative contribution of OPN to collateral formation compared to other targets downstream of H₂O₂, we designed an experiment to add OPN back to the ischemic limb. To do this, we developed a lentivirus to overexpress Myc-tagged OPN (LV-OPN). We then used this lentivirus to perform an add-back experiment to determine what effects observed in our Tg^{SMC-Cat} model were due specifically to the loss of H₂O₂-dependent OPN expression versus the loss of other H₂O₂-dependent proteins. We directly injected the adductor muscles of the IL with either control lentivirus (LV-GFP) or LV-OPN. We verified successful transduction of cells in the adductor muscle by immunofluorescence staining for Myc or GFP (Supplemental Figure 3).²⁹ As expected, the Tg^{SMC-Cat}+LV-GFP treatment group had less reperfusion than the WT+LV-GFP group, such as that observed in Figure 5A. Interestingly, the add-back of OPN to Tg^{SMC-Cat} animals using LV-OPN (Tg^{SMC-Cat}+LV-OPN) restored collateral formation and reperfusion to a level similar to that seen in WT+LV-GFP control animals (Figure 5D-E). These data strongly support OPN as a critical mediator of post-ischemic neo-vascularization.

H₂O₂ Increases OPN Expression In Vitro

Our data demonstrate that ischemia-induced OPN expression in a murine model of HLI is H₂O₂-dependent and that SMC-derived H₂O₂ promotes increased OPN expression in the IL. To determine if H₂O₂ directly mediates an increase in OPN expression, we used an *in vitro* system in which MASMs were quiesced for 48 hours prior to stimulation with 100μM H₂O₂ for 4 hours. Stimulation of MASMs with H₂O₂ significantly increased OPN mRNA expression (Figure 6A), cellular OPN protein expression (Figure 6B), and secreted OPN protein expression (Figure 6C) compared to control. Taken together, these data demonstrate that OPN expression can be directly induced by H₂O₂ *in vitro*.

DISCUSSION

In this study, we demonstrate that ischemia-induced OPN is H₂O₂-dependent and is necessary to promote neo-vascularization. We not only demonstrate that OPN expression in the IL is increased, but that the removal of H₂O₂ via pharmacologic or transgenic approaches significantly blunts H₂O₂-dependent OPN expression *in vivo* and results in substantially impaired reperfusion and collateral formation. Our results define a novel mechanism for the regulation of OPN expression by H₂O₂, demonstrate that H₂O₂-dependent OPN expression is a critical mediator of post-natal neo-vascularization and implicate OPN as a potential therapeutic target for modulating collateral vessel formation.

A recent study provided a direct link between NADPH oxidases, which produce ROS, and post-ischemic neo-vascularization in a murine model of HLI.²³ However, the role of specific ROS species, as well as the major cellular sources of ROS, remains unclear. Superoxide has

been implicated in the process of neo-vascularization,^{23, 37-39} where the contributions of $O_2^{\bullet-}$ as a positive or negative contributor to the neo-vascularization process depends on the overall level of oxidative stress. The role of H_2O_2 in angiogenesis has been studied *in vitro*, where it induces the formation of tube-like structures by endothelial cells¹⁹ and promotes the proliferation and migration of endothelial cells and SMCs.¹³⁻¹⁶ However, a role for H_2O_2 in the process of collateral vessel formation had yet to be established. Our data show that at 5 days post-HLI, H_2O_2 production in the IL of C57Bl/6 animals was significantly increased (Fig. 2B). In contrast, no significant increases in $O_2^{\bullet-}$ were detected in response to ischemia (Fig. 2A). Our data clearly implicate a central role for H_2O_2 in the neo-vascularization process, where both PEG-catalase infused mice and $Tg^{SMC-Cat}$ animals, which have decreased H_2O_2 production (Fig. 3A & 4A), exhibit impaired blood flow and neo-vascularization in response to ischemia (Sup.Fig. 2A and Fig. 5A). A recent study from our laboratory established myeloid lineage cells as one source of H_2O_2 in the collateral formation process.²⁸ The new data presented herein provide evidence that SMC-derived H_2O_2 promotes neo-vascularization, as demonstrated by the impaired reperfusion and collateral formation seen in $Tg^{SMC-Cat}$ mice (Fig. 5A-C). These data provide strong evidence that neo-vascularization in response to ischemia is attributable to the effects of H_2O_2 .

OPN is expressed by multiple cell types including monocytes and macrophages, ECs, and SMCs,⁷ all of which play a role in the neo-vascularization process. OPN mediates several processes relevant to collateral formation, including cell survival,⁸ cell adhesion,^{9, 10} and migration.^{9, 11} Additionally, our lab has previously established OPN as a critical component of the neo-vascularization process, where $OPN^{-/-}$ mice exhibit dramatically impaired collateral formation in response to ischemia.⁵ Our new data show a strong up-regulation of OPN in response to ischemia (Fig. 1). The increase in OPN mRNA levels in response to ischemia at 5 days was >20-fold. Increased OPN mRNA also translated into substantial increases in OPN protein (Fig. 1). Additionally, we present evidence that multiple cells types contribute to ischemia-induced increases in OPN expression (Fig. 1D-F), including macrophages, endothelial cells, and smooth muscle cells. This strong up-regulation in OPN expression in response to ischemia, paired with the lack of collateral formation in $OPN^{-/-}$ mice, define OPN as a critical mediator of the processes required for neo-vascularization. Therefore, it becomes important to fully understand how OPN expression is regulated in this setting and how OPN may function to promote collateral formation.

How OPN functions to increase collateral formation remains largely unknown. One mechanism by which OPN signals is through its RGD domain, which is exposed after OPN cleavage by thrombin or MMPs, and allows OPN to bind multiple integrin subtypes. Another potential mechanism by which OPN may increase collateral formation is through its ability to bind CD44, which does not require OPN cleavage. As shown in Figure 1C, we observe substantial increases in both full-length and cleaved OPN in response to ischemia. However, it remains unclear what functional domains of OPN are required to increase neo-vascularization. Future studies will investigate the precise mechanisms by which OPN increases collateral formation, what protein domains are necessary, and how post-translational modifications alter the ability of OPN to stimulate neo-vascularization.

Little is understood regarding the identity of the specific ROS, $O_2^{\bullet-}$ or H_2O_2 , that regulate OPN expression *in vivo* in response to ischemia. Previous findings suggest a link between ROS and OPN, where in settings in which ROS are increased, such as type 2 diabetes⁴⁰ and atherosclerosis,⁴¹ there is a correlative increase in OPN expression. Similarly, our data show that when H_2O_2 is increased (Fig. 2), there is a correlative increase in OPN in response to ischemia (Fig. 1). To determine if the increase in OPN in response to ischemia was mediated directly by H_2O_2 , we used both pharmacologic and transgenic approaches with our *in vivo*

ischemia model. Catalase, an enzyme that converts H_2O_2 to water and other secondary metabolites, diminishes H_2O_2 levels. To decrease H_2O_2 levels *in vivo*, we infused animals with PEG-Catalase, since the addition of polyethylene glycol has been shown to significantly increase the circulating half-life of the enzyme without impairing enzymatic function.^{42, 43} When H_2O_2 was decreased pharmacologically by PEG-catalase infusion, there were significant decreases in ischemia-induced OPN mRNA and protein expression (Fig. 3). Additionally, when H_2O_2 levels were decreased using SMC catalase overexpressing mice, there was a similar decrease in OPN mRNA and protein expression in response to ischemia (Fig. 4). Several recent publications link ROS to OPN expression in different *in vitro* cell systems, including renal epithelial and vascular smooth muscle cells.²⁴⁻²⁶ Consistent with this, our *in vitro* data also provide evidence that H_2O_2 can directly induce increased OPN expression (Fig. 6). The precise mechanism by which H_2O_2 increases OPN in vascular smooth muscle cells requires further investigation.

Altogether, these data strongly support a direct relationship between H_2O_2 and OPN expression *in vivo*, specifically that H_2O_2 produced in response to ischemia increases OPN expression and that SMCs are one of the contributing sources of H_2O_2 in this model. As evidenced by IF (Fig. 1 D-F), SMCs are but one cell type that contributes to increased OPN production in the IL. The dramatic effects observed in Tg^{SMC-Cat} animals may be due, in part, to SMC-catalase overexpressing cells serving as a sink for H_2O_2 generated by other cell types in response to ischemia, since H_2O_2 is freely diffusible. In both scenarios where H_2O_2 -dependent OPN expression is decreased, there is substantially impaired reperfusion and collateral formation in response to ischemia compared to controls, where OPN expression is maintained and collateral formation is preserved. Furthermore, when OPN was overexpressed in the ischemic limb of Tg^{SMC-Cat} animals using lentivirus, collateral formation and reperfusion was restored to levels similar to those seen in WT+LV-GFP control animals (Fig. 5D-E), further substantiating OPN as a critical mediator of post-ischemic neo-vascularization.

The experiments performed in this study establish that H_2O_2 -dependent OPN is an important mediator of post-ischemic neo-vascularization. One mechanism by which H_2O_2 stimulates collateral vessel formation is through the H_2O_2 -dependent up-regulation of OPN expression, which functions to promote neo-vascularization. Future studies will focus on determining how H_2O_2 regulates OPN expression and defining the pathways activated by H_2O_2 and upstream of OPN. Fully understanding how OPN functions to increase neo-vascularization may ultimately allow for the development of new therapeutics to increase collateral formation in ischemic tissues to restore blood flow and preserve tissue function.

Supplementary Material

Refer to Web version on PubMed Central for supplementary material.

Acknowledgments

We thank Dr. Kerry J. Ressler (Emory University) and Dr. Bernard Lassegue (Emory University) for assistance with lentivirus construct design; Viral Vector Core of the Emory Neuroscience NINDS Core Facilities, funded by grant P30NS055077, for providing the lentivirus vector plasmid; and Drs. Yury A. Bochkov and Ann C. Palmenberg (University of Wisconsin – Madison) for providing the pF/R-wt plasmid containing the WT IRES.

Sources of Funding This work was supported by NIH PO1 HL095070, NIH RO1 HL09058, NIH RO1HL062820 and a post-doctoral grant to Alicia N. Lyle from the American Heart Association.

Non-Standard Abbreviations and Acronyms

DHE	Dihydroethidium
GFP	Green Fluorescent Protein
H₂O₂	Hydrogen Peroxide
HLI	Hind Limb Ischemia
HPLC	High-performance Liquid Chromatography
IF	Immunofluorescence
IL	Ischemic Limb
IRES	Internal Ribosomal Entry Site
LDPI	LASER Doppler Perfusion Imaging
LV	Lentivirus
NIL	Non-ischemic Limb
O₂^{•-}	Superoxide
OPN	Osteopontin
PEG	Polyethylene Glycol
RGD	Arginine-Glycine-Aspartate
ROS	Reactive Oxygen Species
SMCs	Smooth Muscle Cells

REFERENCES

1. Sabia PJ, Powers ER, Jayaweera AR, Ragosta M, Kaul S. Functional significance of collateral blood flow in patients with recent acute myocardial infarction. A study using myocardial contrast echocardiography. *Circulation*. 1992; 85:2080–2089. [PubMed: 1591827]
2. Morimoto J, Kon S, Matsui Y, Uede T. Osteopontin; as a target molecule for the treatment of inflammatory diseases. *Curr Drug Targets*. 11:494–505. [PubMed: 20196720]
3. Wang KX, Denhardt DT. Osteopontin: Role in immune regulation and stress responses. *Cytokine Growth Factor Rev*. 2008; 19:333–345. [PubMed: 18952487]
4. Duvall CL, Taylor WR, Weiss D, Wojtowicz AM, Guldberg RE. Impaired angiogenesis, early callus formation, and late stage remodeling in fracture healing of osteopontin-deficient mice. *J Bone Miner Res*. 2007; 22:286–297. [PubMed: 17087627]
5. Duvall CL, Weiss D, Robinson ST, Alameddine FM, Guldberg RE, Taylor WR. The role of osteopontin in recovery from hind limb ischemia. *Arterioscler Thromb Vasc Biol*. 2008; 28:290–295. [PubMed: 18006856]
6. Myers DL, Harmon KJ, Lindner V, Liaw L. Alterations of arterial physiology in osteopontin-null mice. *Arterioscler Thromb Vasc Biol*. 2003; 23:1021–1028. [PubMed: 12714436]
7. O'Brien ER, Garvin MR, Stewart DK, Hinohara T, Simpson JB, Schwartz SM, Giachelli CM. Osteopontin is synthesized by macrophage, smooth muscle, and endothelial cells in primary and restenotic human coronary atherosclerotic plaques. *Arterioscler Thromb*. 1994; 14:1648–1656. [PubMed: 7918316]
8. Scatena M, Almeida M, Chaisson ML, Fausto N, Nicosia RF, Giachelli CM. Nf-kappab mediates alphavbeta3 integrin-induced endothelial cell survival. *J Cell Biol*. 1998; 141:1083–1093. [PubMed: 9585425]
9. Liaw L, Almeida M, Hart CE, Schwartz SM, Giachelli CM. Osteopontin promotes vascular cell adhesion and spreading and is chemotactic for smooth muscle cells in vitro. *Circ Res*. 1994; 74:214–224. [PubMed: 8293561]

10. Liaw L, Skinner MP, Raines EW, Ross R, Cheresh DA, Schwartz SM, Giachelli CM. The adhesive and migratory effects of osteopontin are mediated via distinct cell surface integrins. Role of alpha v beta 3 in smooth muscle cell migration to osteopontin in vitro. *J Clin Invest.* 1995; 95:713–724. [PubMed: 7532190]
11. Giachelli CM, Lombardi D, Johnson RJ, Murry CE, Almeida M. Evidence for a role of osteopontin in macrophage infiltration in response to pathological stimuli in vivo. *Am J Pathol.* 1998; 152:353–358. [PubMed: 9466560]
12. Liaw L, Birk DE, Ballas CB, Whitsitt JS, Davidson JM, Hogan BL. Altered wound healing in mice lacking a functional osteopontin gene (spp1). *J Clin Invest.* 1998; 101:1468–1478. [PubMed: 9525990]
13. Scatena M, Liaw L, Giachelli CM. Osteopontin: A multifunctional molecule regulating chronic inflammation and vascular disease. *Arterioscler Thromb Vasc Biol.* 2007; 27:2302–2309. [PubMed: 17717292]
14. Weber GF, Ashkar S, Glimcher MJ, Cantor H. Receptor-ligand interaction between cd44 and osteopontin (eta-1). *Science.* 1996; 271:509–512. [PubMed: 8560266]
15. Weber GF, Zawaideh S, Hikita S, Kumar VA, Cantor H, Ashkar S. Phosphorylation-dependent interaction of osteopontin with its receptors regulates macrophage migration and activation. *J Leukoc Biol.* 2002; 72:752–761. [PubMed: 12377945]
16. Liaw L, Lombardi DM, Almeida MM, Schwartz SM, deBlois D, Giachelli CM. Neutralizing antibodies directed against osteopontin inhibit rat carotid neointimal thickening after endothelial denudation. *Arterioscler Thromb Vasc Biol.* 1997; 17:188–193. [PubMed: 9012655]
17. Shinohara ML, Kim HJ, Kim JH, Garcia VA, Cantor H. Alternative translation of osteopontin generates intracellular and secreted isoforms that mediate distinct biological activities in dendritic cells. *Proc Natl Acad Sci U S A.* 2008; 105:7235–7239. [PubMed: 18480255]
18. Zohar R, Suzuki N, Suzuki K, Arora P, Glogauer M, McCulloch CA, Sodek J. Intracellular osteopontin is an integral component of the cd44-erm complex involved in cell migration. *J Cell Physiol.* 2000; 184:118–130. [PubMed: 10825241]
19. Maulik N, Das DK. Redox signaling in vascular angiogenesis. *Free Radic Biol Med.* 2002; 33:1047–1060. [PubMed: 12374616]
20. Martin AS, Griendling KK. Redox control of vascular smooth muscle migration. *Antioxid Redox Signal.*
21. Ushio-Fukai M. Redox signaling in angiogenesis: Role of nadph oxidase. *Cardiovasc Res.* 2006; 71:226–235. [PubMed: 16781692]
22. Griendling KK, Ushio-Fukai M. Redox control of vascular smooth muscle proliferation. *J Lab Clin Med.* 1998; 132:9–15. [PubMed: 9665366]
23. Tojo T, Ushio-Fukai M, Yamaoka-Tojo M, Ikeda S, Patrushev N, Alexander RW. Role of gp91phox (nox2)-containing nad(p)h oxidase in angiogenesis in response to hindlimb ischemia. *Circulation.* 2005; 111:2347–2355. [PubMed: 15867174]
24. Hu T, Luan R, Zhang H, Lau WB, Wang Q, Zhang Y, Wang HC, Tao L. Hydrogen peroxide enhances osteopontin expression and matrix metalloproteinase activity in aortic vascular smooth muscle cells. *Clin Exp Pharmacol Physiol.* 2009; 36:626–630. [PubMed: 19076167]
25. Maziere C, Gomila C, Maziere JC. Oxidized low-density lipoprotein increases osteopontin expression by generation of oxidative stress. *Free Radic Biol Med.* 2010; 48:1382–1387. [PubMed: 20211246]
26. Umekawa T, Tsuji H, Uemura H, Khan SR. Superoxide from nadph oxidase as second messenger for the expression of osteopontin and monocyte chemoattractant protein-1 in renal epithelial cells exposed to calcium oxalate crystals. *BJU Int.* 2009; 104:115–120. [PubMed: 19220254]
27. Zhang Y, Griendling KK, Dikalova A, Owens GK, Taylor WR. Vascular hypertrophy in angiotensin ii-induced hypertension is mediated by vascular smooth muscle cell-derived h2o2. *Hypertension.* 2005; 46:732–737. [PubMed: 16172434]
28. Hodara R, Weiss D, Joseph G, Velasquez-Castano JC, Landazuri N, Han JW, Yoon YS, Taylor WR. Overexpression of catalase in myeloid cells causes impaired postischemic neovascularization. *Arterioscler Thromb Vasc Biol.* 2011

29. Heldt SA, Stanek L, Chhatwal JP, Ressler KJ. Hippocampus-specific deletion of *bdnf* in adult mice impairs spatial memory and extinction of aversive memories. *Mol Psychiatry*. 2007; 12:656–670. [PubMed: 17264839]
30. Tiscornia G, Singer O, Ikawa M, Verma IM. A general method for gene knockdown in mice by using lentiviral vectors expressing small interfering rna. *Proc Natl Acad Sci U S A*. 2003; 100:1844–1848. [PubMed: 12552109]
31. Naldini L, Blomer U, Gage FH, Trono D, Verma IM. Efficient transfer, integration, and sustained long-term expression of the transgene in adult rat brains injected with a lentiviral vector. *Proc Natl Acad Sci U S A*. 1996; 93:11382–11388. [PubMed: 8876144]
32. Bochkov YA, Palmenberg AC. Translational efficiency of emcv ires in bicistronic vectors is dependent upon ires sequence and gene location. *Biotechniques*. 2006; 41:283–284. 286, 288 passim. [PubMed: 16989088]
33. Miyoshi H, Blomer U, Takahashi M, Gage FH, Verma IM. Development of a self-inactivating lentivirus vector. *J Virol*. 1998; 72:8150–8157. [PubMed: 9733856]
34. Pfeifer A, Brandon EP, Kootstra N, Gage FH, Verma IM. Delivery of the cre recombinase by a self-deleting lentiviral vector: Efficient gene targeting in vivo. *Proc Natl Acad Sci U S A*. 2001; 98:11450–11455. [PubMed: 11553794]
35. Lyle AN, Deshpande NN, Taniyama Y, Seidel-Rogol B, Pounkova L, Du P, Papaharalambus C, Lassegue B, Griendling KK. Poldip2, a novel regulator of nox4 and cytoskeletal integrity in vascular smooth muscle cells. *Circ Res*. 2009; 105:249–259. [PubMed: 19574552]
36. Kazanecki CC, Uzwiak DJ, Denhardt DT. Control of osteopontin signaling and function by post-translational phosphorylation and protein folding. *J Cell Biochem*. 2007; 102:912–924. [PubMed: 17910028]
37. Haddad P, Dussault S, Groleau J, Turgeon J, Michaud SE, Menard C, Perez G, Maingrette F, Rivard A. Nox2-containing nadph oxidase deficiency confers protection from hindlimb ischemia in conditions of increased oxidative stress. *Arterioscler Thromb Vasc Biol*. 2009; 29:1522–1528. [PubMed: 19574557]
38. Kim HW, Lin A, Guldberg RE, Ushio-Fukai M, Fukai T. Essential role of extracellular sod in reparative neovascularization induced by hindlimb ischemia. *Circ Res*. 2007; 101:409–419. [PubMed: 17601801]
39. Ushio-Fukai M, Tang Y, Fukai T, Dikalov SI, Ma Y, Fujimoto M, Quinn MT, Pagano PJ, Johnson C, Alexander RW. Novel role of gp91(phox)-containing nad(p)h oxidase in vascular endothelial growth factor-induced signaling and angiogenesis. *Circ Res*. 2002; 91:1160–1167. [PubMed: 12480817]
40. San Martin A, Du P, Dikalova A, Lassegue B, Aleman M, Gongora MC, Brown K, Joseph G, Harrison DG, Taylor WR, Jo H, Griendling KK. Reactive oxygen species-selective regulation of aortic inflammatory gene expression in type 2 diabetes. *Am J Physiol Heart Circ Physiol*. 2007; 292:H2073–2082. [PubMed: 17237245]
41. Bruemmer D, Collins AR, Noh G, Wang W, Territo M, Arias-Magallona S, Fishbein MC, Blaschke F, Kintscher U, Graf K, Law RE, Hsueh WA. Angiotensin ii-accelerated atherosclerosis and aneurysm formation is attenuated in osteopontin-deficient mice. *J Clin Invest*. 2003; 112:1318–1331. [PubMed: 14597759]
42. Abuchowski A, McCoy JR, Palczuk NC, van Es T, Davis FF. Effect of covalent attachment of polyethylene glycol on immunogenicity and circulating life of bovine liver catalase. *J Biol Chem*. 1977; 252:3582–3586. [PubMed: 16907]
43. Beckman JS, Minor RL Jr, White CW, Repine JE, Rosen GM, Freeman BA. Superoxide dismutase and catalase conjugated to polyethylene glycol increases endothelial enzyme activity and oxidant resistance. *J Biol Chem*. 1988; 263:6884–6892. [PubMed: 3129432]

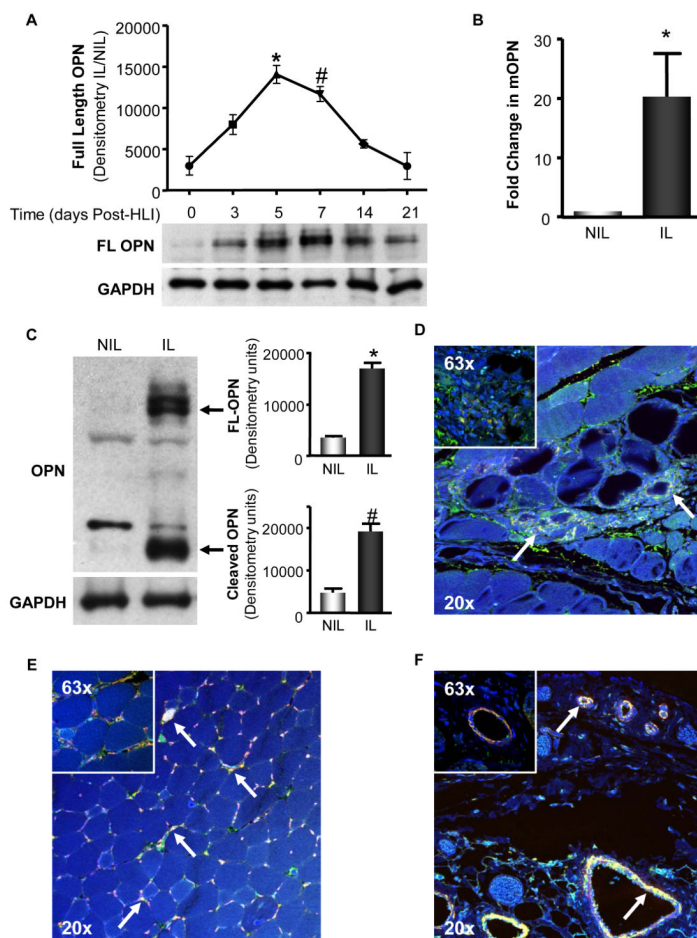


Figure 1. Hind Limb Ischemia Increases OPN expression in the Proximal Region of the Ischemic Limb – Contributing Cell Types Include Macrophages, Endothelial Cells, and Smooth Muscle Cells

Femoral artery ligation was performed on C57Bl/6 mice and OPN expression was assessed in the adductor muscles of the non-ischemic (NIL) and ischemic limbs (IL) at the time points indicated. **A.** Full-length (FL) OPN protein expression in the IL was measured by Western blot (WB) at 0, 3, 5, 7, 14, and 21 days post-surgery. (* $p < 0.05$ vs. day 0, 3, 14, & 21; # $p < 0.05$ vs. day 0, 14, & 21; $n = 3-4$). GAPDH demonstrates equal loading. **B.** OPN mRNA was assessed by qRT-PCR (* $p < 0.05$, $n = 3$). **C.** FL and cleaved OPN protein expression at 5d was measured by WB. (FL, * $p < 0.001$; cleaved, # $p < 0.05$; $n = 4$). GAPDH demonstrates equal loading. **D-F.** OPN expression and distribution was assessed in the adductor muscles of the IL at 5 days in C57Bl/6 mice. In all panels, DAPI appears blue and stains the nuclei, OPN appears green, the designated cell marker appears as red, and co-localization is yellow and denoted with arrows. All panels include an image taken at 20x, to show anatomical structure, and 63x, to show co-localization detail. **D.** OPN (green) co-localizes with Mac3 (red), a marker for macrophages. **E.** OPN (green) co-localizes with lectin (red), a marker for endothelial cells. **F.** OPN (green) co-localizes with smooth muscle α -actin (red), a marker for SMCs. Bars are means \pm S.E.M.

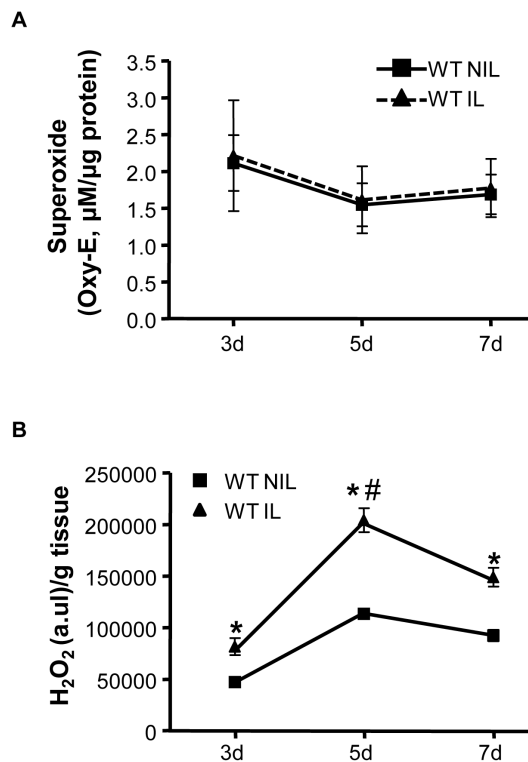


Figure 2. Hind Limb Ischemia Increases ROS in the Proximal Region of the Ischemic Hind Limb
 ROS production was assessed in the adductor muscles of the non-ischemic (NIL) and ischemic limbs (IL) of C57Bl/6 mice at postoperative day 3, 5, and 7. **A.** $O_2^{\bullet-}$ production was measured using DHE-HPLC. (ns; n=5-6) **B.** The Amplex Red Assay was used to measure H_2O_2 levels. H_2O_2 measurements were normalized to tissue wet weight. H_2O_2 was increased in the IL compared to the NIL at 3, 5, and 7 days (* $p < 0.001$), with a peak at 5d (# $p < 0.05$ vs. 3d). n=3-6. Bars are means \pm S.E.M.

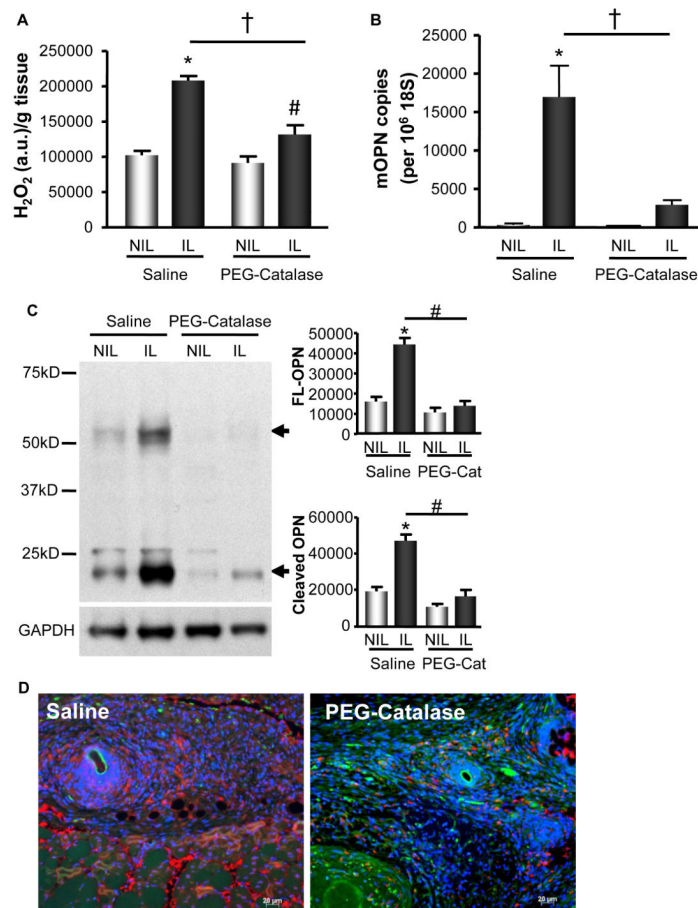


Figure 3. OPN Expression in the Proximal Region of the Ischemic Limb is H₂O₂-dependent
H₂O₂ production and OPN expression were measured in the adductor muscles of the non-ischemic (NIL) and ischemic limbs (IL) at postoperative day 5 in C57Bl/6 mice infused with Saline or 10,000 U/kg/day PEG-Catalase (PEG-Cat). **A.** H₂O₂ was measured by Amplex Red Assay. H₂O₂ was increased in the IL of both treatment groups (*p<0.001 vs. Saline NIL; #p<0.05 vs. PEG-Catalase NIL); however, PEG-catalase blunted ischemia-induced H₂O₂ compared to control (†p<0.001). n=5. **B.** OPN mRNA levels were measured by qRT-PCR. OPN was increased in the IL of saline controls (*p<0.001 vs. Saline NIL), but not animals infused with PEG-catalase. PEG-catalase treatment blocked increased OPN mRNA in the IL (†p<0.01). n=5. **C.** Full-length (FL) and cleaved OPN protein expression in the IL of saline infused animals were increased at 5d by WB analysis (FL, *p<0.001; cleaved, *p<0.001; n=8). PEG-catalase (PEG-Cat) treatment blunted this increase (FL, #p<0.0001; cleaved, #p<0.0001; n=8). GAPDH demonstrates equal loading. **D.** PEG-catalase decreased OPN protein expression in the IL compared to control at 5d, as detected by immunofluorescence. Blue=DAPI-nuclei, Red=OPN, Green=autofluorescence. Bars are means ± S.E.M.

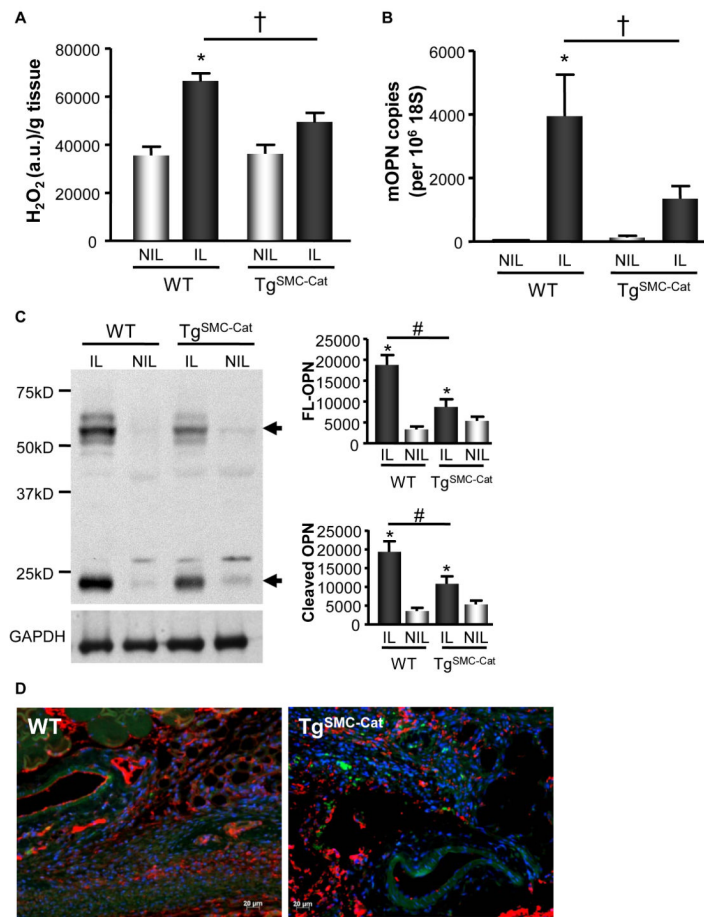


Figure 4. OPN Expression in the Proximal Region of the Ischemic Limb is Decreased by SMC-specific Catalase Overexpression

H₂O₂ production and OPN expression were measured at postoperative day 5 days in Tg^{SMC-Cat} or wild-type (WT) littermates. **A.** H₂O₂ production was increased in the IL of WT and Tg^{SMC-Cat} animals, as measured by Amplex Red (*p<0.001); however, Tg^{SMC-Cat} animals exhibit decreased H₂O₂ production in the IL compared to WT (†p<0.0001). H₂O₂ measurements were normalized to tissue wet weight. n=5. **B.** OPN mRNA levels were increased in the WT IL (*p<0.001 vs. NIL); however, OPN mRNA levels in the Tg^{SMC-Cat} IL was not increased compared to the NIL. Tg^{SMC-Cat} animals had decreased OPN mRNA in the IL compared to WT (†p<0.05). n=6. **C.** Full-length (FL) and cleaved OPN protein expression in the WT IL was increased at 5d by WB analysis (FL, *p<0.001; cleaved, *p<0.001; n=5). This increase was blunted in Tg^{SMC-Cat} animals (FL, #p<0.01; cleaved, #p<0.01; n=5). GAPDH demonstrates equal loading. **D.** OPN expression in the Tg^{SMC-Cat} IL is decreased compared to WT IL at 5d by immunofluorescence. Blue=DAPI - nuclei, Red=OPN, Green=autofluorescence. Bars are means ± S.E.M.

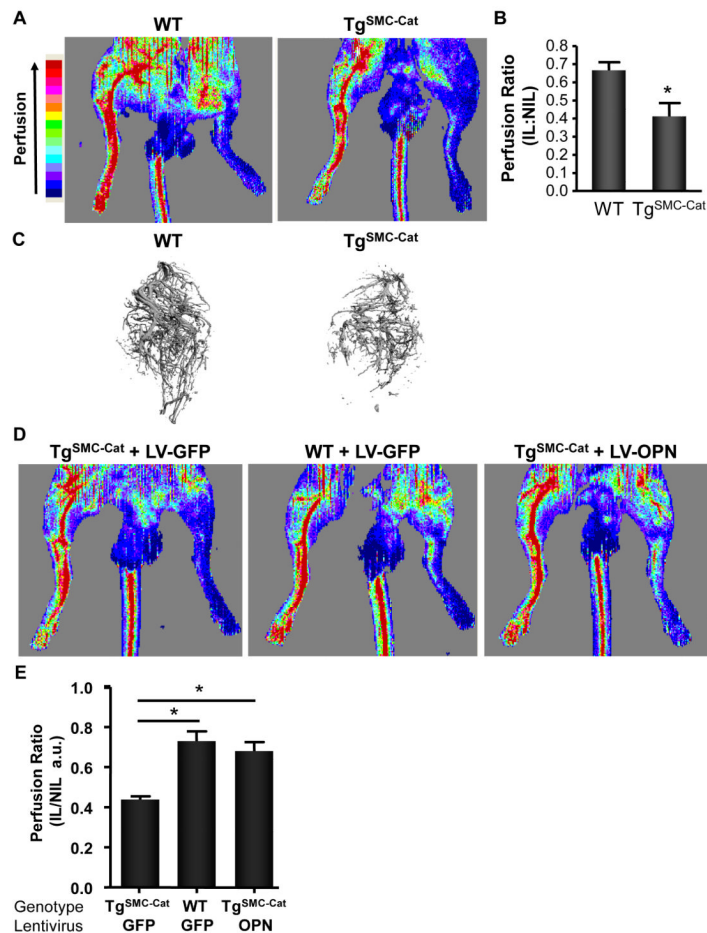


Figure 5. H₂O₂-dependent OPN Mediates Collateral Formation

LASER Doppler Perfusion Imaging (LDPI) was used to evaluate perfusion and Micro-CT to quantify collateral formation in the IL. Perfusion and collateral formation was assessed in the proximal regions of the IL and normalized to the NIL. All measurements were performed at 5d post-surgery. Ischemic legs were compared between treatment groups. **A.** Representative LDPI tracings from WT and Tg^{SMC-Cat} animals at day 5. **B.** Quantitative analysis of WT and Tg^{SMC-Cat} LDPI tracings (*p<0.05, n=5). **C.** Representative Micro-CT angiographs from WT and Tg^{SMC-Cat} mice at postoperative day 5. To determine the relative contribution of OPN to collateral formation compared to other H₂O₂-dependent pathways, we performed an OPN add-back experiment. Tg^{SMC-Cat}+LV-GFP treatment group had less reperfusion than WT+LV-GFP mice. Add-back of OPN to Tg^{SMC-Cat} mice using LV-OPN (Tg^{SMC-Cat}+LV-OPN) restored collateral formation and perfusion to the level of WT animals. **D.** Representative LDPI tracings from WT+LV-GFP control, Tg^{SMC-Cat}+LV-GFP, and Tg^{SMC-Cat}+LV-OPN treated animals. **E.** Quantitative analysis of WT+LV-GFP control, Tg^{SMC-Cat}+LV-GFP, and Tg^{SMC-Cat}+LV-OPN LDPI tracings. (*p<0.001 vs. Tg^{SMC-Cat}+LV-GFP, n=6). Bars are means ± S.E.M.

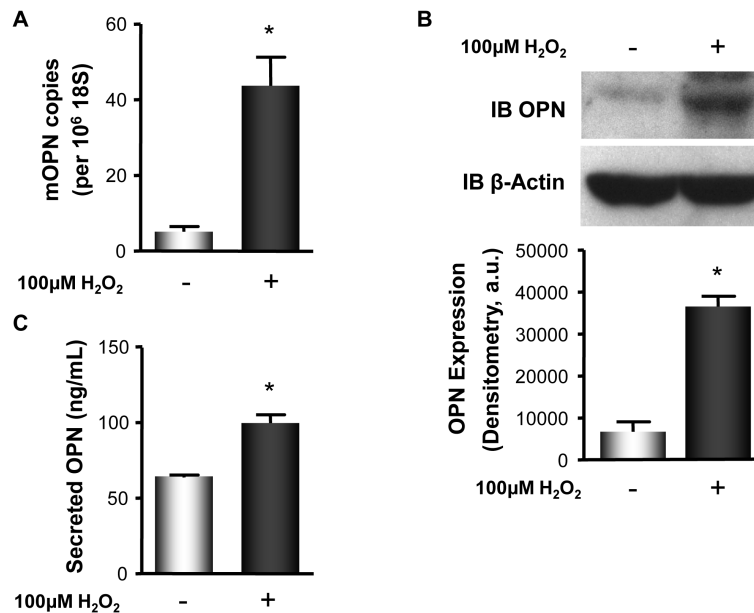


Figure 6. H₂O₂ Increases OPN Expression in Mouse Aortic Smooth Muscle Cells

Murine SMCs were used as an *in vitro* system. SMCs were quiesced for 48 hours prior to no treatment (–) or stimulation (+) with 100 µM H₂O₂ for 4 hours. Cells were harvested for mRNA and protein and DMEM collected to assess secreted OPN by ELISA. **A.** H₂O₂ stimulation increased OPN mRNA expression (*p<0.01), **B.** cellular OPN protein expression (*p<0.0001), measured by WB, and **C.** secreted OPN protein expression, measured by ELISA (*p<0.001). Bars are means ± S.E.M., n=4.